


Data-Driven Optimization of UPQC Performance for Solar PV Systems in Weak Grids Using Simulation and Predictive Modeling

Rajasree R^{1,*}, Lakshmi D.², M. Batumalay³ 

^{1,2}AMET University, Tamil Nadu, India

³Faculty of Data Science and IT, INTI International University, Nilai, N. Sembilan, Malaysia

³Centre for Data Science and Sustainable Technologies, INTI International University, Nilai, N. Sembilan, Malaysia

(Received: January 5, 2025; Revised: February 10, 2025; Accepted: May 10, 2025; Available online: July 19, 2025)

Abstract

The integration of solar photovoltaic (PV) systems into weak power grids presents significant challenges due to low short circuit ratios (SCR), resulting in voltage instability, high harmonic distortion, and diminished fault tolerance. This study proposes a data-driven framework to enhance grid stability and power quality by employing a Unified Power Quality Conditioner (UPQC) integrated with Proportional-Integral (PI) controllers. A comprehensive simulation model was developed using MATLAB/Simulink and validated through hardware-in-the-loop (HIL) experiments. Key electrical performance metrics—such as voltage profiles, total harmonic distortion (THD), and reactive power—were collected and analyzed. To enhance system insight, the dataset was further processed using statistical analysis and predictive modeling techniques to evaluate control response under varying solar irradiance and load conditions. The results demonstrate that the UPQC system maintains stable voltage, reduces THD to within IEEE-519 standards, and improves power factor to 0.98. This research highlights the potential of combining power electronics control with data-centric evaluation to ensure reliable renewable energy integration in weak grid environments. The proposed system contributes toward developing intelligent grid-support solutions for sustainable energy transitions and process innovation.

Keywords: Unified Power Quality Conditioner (UPQC), Power Quality, Total Harmonic Distortion (THD), Reactive Power Compensation, Process Innovation

1. Introduction

The global shift toward sustainable and environmentally friendly energy systems has significantly increased the penetration of Renewable Energy Sources (RES), particularly solar and wind power, into modern power grids. While this transition reduces dependence on fossil fuels, it also introduces critical operational challenges—especially in weak grids, which are characterized by high impedance, low short-circuit capacity, and limited reactive power support. These characteristics make weak grids highly vulnerable to voltage instability, harmonic distortion, and frequency deviation [1], [2].

Among the key issues encountered is the integration of solar PV systems, which can severely degrade power quality and stability when connected to weak grids, particularly when the SCR falls below 3. At high levels of renewable penetration (exceeding 30–40% of the load), such systems exhibit frequent voltage sags, swells, and THD, complicating grid operation and reliability [3], [4]. Addressing these nonlinear and dynamic behaviours necessitates advanced power conditioning systems and intelligent control strategies.

This research investigates the role of the UPQC as a dual-compensation system—comprising series and shunt converters—for real-time mitigation of both voltage- and current-related power disturbances. Unlike traditional Flexible AC Transmission System (FACTS) devices that focus on isolated issues, the UPQC provides simultaneous compensation for voltage instability, reactive power imbalances, and harmonic distortions [5], [6]. Its comprehensive control framework enables performance enhancement across both the supply and load sides of the network.

To analyze the UPQC's performance, a simulation environment using MATLAB/Simulink was developed and complemented by HIL testing. Key performance indicators—such as voltage regulation, power factor correction, and

*Corresponding author: Rajasree R. (raji.sree1988@gmail.com)

 DOI: <https://doi.org/10.47738/jads.v6i3.742>

This is an open access article under the CC-BY license (<https://creativecommons.org/licenses/by/4.0/>).

© Authors retain all copyrights

THD—were monitored under varying solar irradiance and load conditions [7], [8]. Beyond engineering simulations, this study integrates data analysis techniques to model system behavior, assess control responsiveness, and quantify the stability margin improvements. By framing simulation output as time-series data, we enable predictive modelling of voltage performance and THD under uncertain renewable conditions [9].

This interdisciplinary approach bridges control engineering and data science, offering valuable insights for grid operators, engineers, and researchers in developing resilient and intelligent renewable energy infrastructures. As energy systems evolve toward smart grids, the integration of control devices like UPQC, combined with data-driven analysis, becomes critical for ensuring reliable and high-quality power delivery in weak grid environments [10].

2. UPQC

The UPQC is a widely adopted device in the category of FACTS used to enhance the integration of RES into weak distribution grids. These weak grids, characterized by high impedance and limited short-circuit capacity, struggle with voltage instability, harmonic distortion, and insufficient reactive power support when faced with fluctuating power injections from intermittent energy sources like solar and wind [11], [12]. To overcome these issues, the UPQC provides comprehensive power quality compensation by simultaneously mitigating both voltage- and current-related disturbances [13]. Figure 1 show the block diagram of UPQC that used in this research.

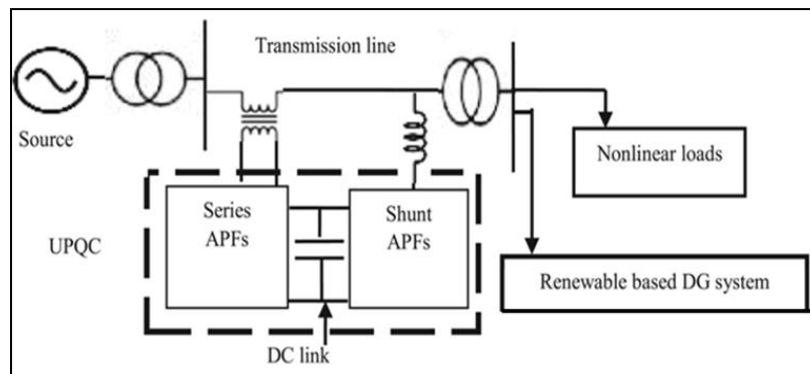


Figure 1. Block Diagram of UPQC (FACTS Device)

The UPQC integrates two core components: a series converter and a shunt converter, which work in tandem to stabilize power flow. The series converter addresses supply-side problems such as voltage sags, swells, and waveform distortions by injecting controlled voltages through coupling transformers. Control strategies commonly used include the Synchronous Reference Frame (SRF) theory and Space Vector Modulation (SVM), which help generate accurate reference voltages for abnormal grid conditions [14], [15].

On the demand side, the shunt converter is connected at the Point of Common Coupling (PCC) and compensates for load harmonics, reactive power, and voltage regulation. It mimics the operation of Active Power Filters and STATCOMs by injecting currents calculated through SRF or p-q theory methods. The DC-link voltage is maintained using a dual-loop control system: an outer loop for voltage regulation and an inner loop for current tracking [16], [17]. This combined architecture allows the UPQC to enhance both voltage and current quality parameters across the grid.

As reported in several studies, the UPQC plays a key role in counteracting the variability of RES, especially in weak grids where frequent changes in irradiance and load can degrade system performance. Fluctuations in solar PV output lead to voltage and frequency swings, increasing the likelihood of power quality violations and equipment failure [18], [19]. By providing reactive power support and harmonic compensation, the UPQC ensures compliance with power quality standards such as IEEE-519 and helps maintain a stable power factor close to unity [20].

Recent innovations have explored the integration of UPQC with Energy Storage Systems (ESS) to allow for temporary energy buffering and improved frequency regulation in weak grids [21]. Such hybrid systems are gaining traction in rural electrification and microgrid applications, where infrastructure limitations and high-RES penetration require fast-acting and adaptive quality control solutions [22], [23].

The advancement of power electronics and embedded control algorithms has further enabled the UPQC to be combined with data-driven control strategies, such as model predictive control (MPC), Kalman filtering, and machine learning

for real-time voltage forecasting [24], [25]. These enhancements pave the way for next-generation UPQC systems that not only react to disturbances but proactively manage power quality using predictive insights.

3. Methodology

3.1. System Overview

The proposed system integrates a PV generation unit with a UPQC to enhance power quality in weak grid networks. The architecture includes a DC-side voltage regulation stage using a Cuk–SEPIC converter, an AC-side compensation system via UPQC, and a feedback control mechanism for dynamic adaptation. A schematic representation is shown in figure 2.

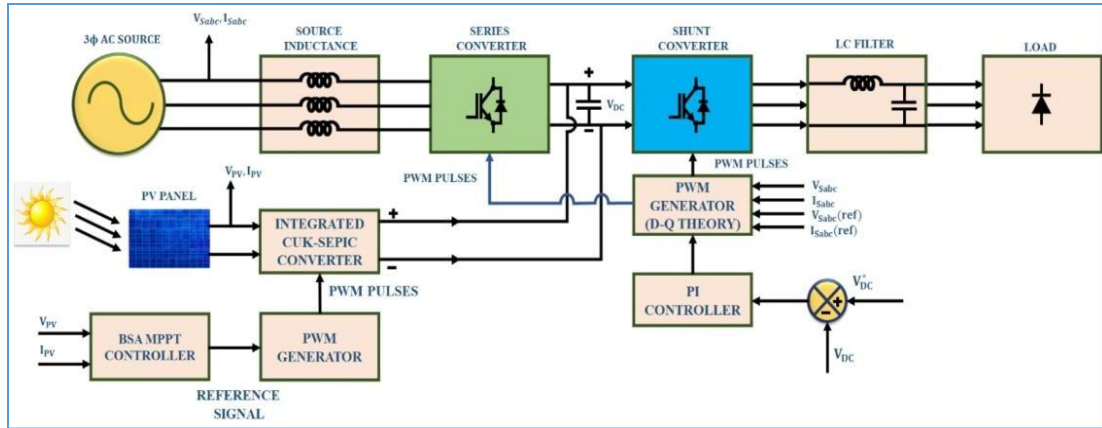


Figure 2. Control Methodology for Weak Grid Integrated Solar PV System

3.2. DC Power Conditioning with Cuk–SEPIC Converter

The solar PV module generates variable DC voltage due to changing irradiance and temperature. A combined Cuk–SEPIC converter stabilizes this voltage. The Cuk stage provides continuous input/output current and reduced EMI, while the SEPIC section ensures a non-inverting and flexible output voltage. The average output voltage V_{out} is related to the input voltage V_{in} and the PWM duty cycle D by:

$$V_{out} = \frac{D}{1-D} \cdot V_{in} \quad (1)$$

An MPPT controller based on Best Slope Approximation (BSA) algorithm maximizes the extracted power from the PV array using the relation:

$$P = V \cdot I \quad (2)$$

The controller continuously adjusts the duty cycle to track the optimal operating point under varying solar conditions [9].

3.3. UPQC Compensation Operation

The UPQC consists of a series converter and a shunt converter. The series converter injects voltage to correct supply-side issues such as voltage sags, swells, and unbalances. The compensation voltage V_{inj} is calculated as:

$$V_{inj} = V_{ref} - V_{grid} \quad (3)$$

The shunt converter compensates for harmonic current and manages reactive power. It also maintains a stable DC-link voltage. Control is based on the transformation of three-phase voltages into the d–q reference frame using Park transformation:

$$\begin{matrix} V_d \\ V_q \\ V_0 \end{matrix} = \frac{2}{3} \begin{matrix} \cos \theta & \cos(\theta - 120^\circ) & \cos(\theta + 120^\circ) \\ \sin \theta & \sin(\theta - 120^\circ) & \sin(\theta + 120^\circ) \\ \frac{1}{2} & \frac{1}{2} & \frac{1}{2} \end{matrix} \begin{matrix} V_a \\ V_b \\ V_c \end{matrix} \quad (4)$$

This transformation enables accurate harmonic detection and decoupling of active and reactive power components [11], [21].

3.4. PI Control and PWM Signal Generation

The DC-link voltage is regulated using a PI controller. The control signal $u(t)$ is generated based on the error $e(t)$ between the reference and actual voltage:

$$e(t) = V_{dc}^{ref} - V_{dc}(t) \quad (5)$$

$$u(t) = K_p \cdot e(t) + K_i \cdot \int e(t) dt \quad (6)$$

The PI output modifies the duty cycle of the PWM signals used to control both converters [13]. An LC filter is added at the output stage to eliminate high-frequency harmonics, ensuring sinusoidal voltage and current delivery that meets IEEE-519 harmonic distortion standards [11].

3.5. System Deployment Context

This PV–UPQC system targets deployment in microgrids, rural electrification schemes, and other weak-grid scenarios with high renewable penetration. The system is capable of adapting to real-time disturbances in solar irradiance and load demand. Smart grid compatibility is supported, enabling future enhancement through predictive analytics, cloud-based monitoring, and intelligent energy dispatch [17].

4. PI Controller Technique

The PI controller is a widely adopted feedback control mechanism in power electronics and automation systems. It regulates system output by continuously minimizing the error between a reference signal and the actual output, ensuring stable and accurate operation [19]. As shown in figure 3, the PI controller structure consists of two key components: a proportional element that provides immediate correction based on present error, and an integral element that accumulates past errors to eliminate steady-state deviations.

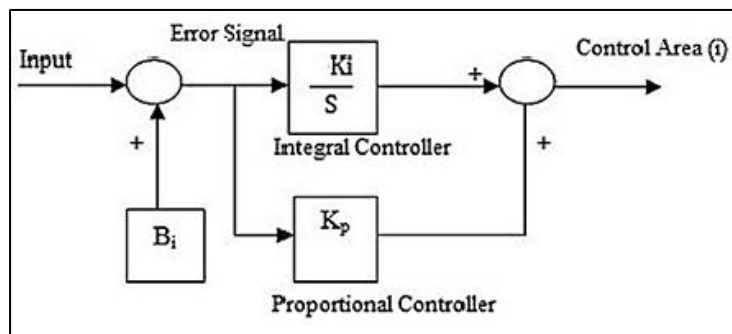


Figure 3. Block Diagram of PI Controller Technique

This combination enables the controller to deliver fast system response and long-term accuracy. Unlike PID controllers, the PI controller excludes the derivative term, which simplifies its design and reduces sensitivity to electrical noise—making it ideal for power converter systems operating in real-world grid conditions [20]. In weak grids, where voltage instability and poor power quality are common due to intermittent solar generation and high system impedance, the PI controller plays a critical role. It is implemented to maintain a stable DC-link voltage between the UPQC’s series and shunt converters, ensuring proper energy transfer from the solar PV array to the grid [6], [12].

The PI controller dynamically adjusts control signals to accommodate changes in irradiance or load, stabilizing the voltage output and enabling the UPQC to perform functions such as harmonic suppression, reactive power compensation, and power factor correction [13]. These capabilities are essential for maintaining power quality in renewable-integrated weak distribution systems. The control signal generated by the PI controller is used by the Pulse Width Modulation (PWM) module to operate the UPQC's converters. This closed-loop control approach allows the system to respond rapidly to transient disturbances while maintaining consistent performance during steady-state operation. Through its integration with the overall UPQC framework, the PI controller ensures that power delivered to the load remains within voltage and harmonic limits, thereby supporting reliable and stable power delivery in compliance with IEEE-519 standards.

5. Simulation Results and Discussion

This study conducted detailed simulations to evaluate the performance of the proposed UPQC system integrated with a PV source under weak grid conditions. The simulations were implemented using MATLAB/Simulink, with a SCR of 2.5 used to represent a weak distribution network. The system operated at a grid voltage of 415 V and a frequency of 50 Hz. The PV array consisted of two strings of eight modules each, totaling 250 MW capacity with 30 V per module. The connected load was modeled as a dynamic, non-linear, and partially resistive load. The total simulation time was 5 seconds, sampled at 0.5 millisecond intervals.

Time-series output from the simulation, including voltage, current, real and reactive power, power factor, and total harmonic distortion (THD), was exported in CSV format for further data analysis using Python libraries such as pandas, matplotlib, and scikit-learn. The collected dataset consisted of over 10,000 entries, enabling a comprehensive statistical and predictive evaluation of system performance.

Under baseline conditions—when the UPQC was not active—the system experienced clear signs of instability. Figure 4 displays the output voltage waveform, where voltage dips and harmonic oscillations are prevalent. These irregularities are symptomatic of weak grid behavior and directly affect the reliability of connected equipment. Figure 5 shows the corresponding current waveform, which is non-sinusoidal and exhibits clear evidence of harmonic content. Figure 6 illustrates the real and reactive power behavior during this period. The real power fluctuates sharply, while reactive power remains relatively high and lagging, indicating inefficient power transfer and poor power factor. Under these conditions, the power factor remains at approximately 0.82, and the THD reaches 8.5%, which exceeds the maximum allowable threshold as defined by IEEE-519 standards.

Figure 4 illustrates the voltage waveform delivered to the load when the UPQC controller is inactive. The waveform clearly deviates from an ideal sinusoidal pattern and exhibits frequent voltage sags and swells. These variations are symptomatic of a weak grid environment where the voltage source lacks the stiffness required to support sudden changes in load or generation. This condition often arises when the grid has a low SCR, as in this simulation case with $SCR = 2.5$. The waveform also reveals high-frequency distortions due to unfiltered harmonics introduced by the power electronic converters of the solar PV system. The poor voltage regulation observed here not only reduces energy delivery efficiency but also places connected loads at risk of malfunction or degradation due to irregular supply conditions.

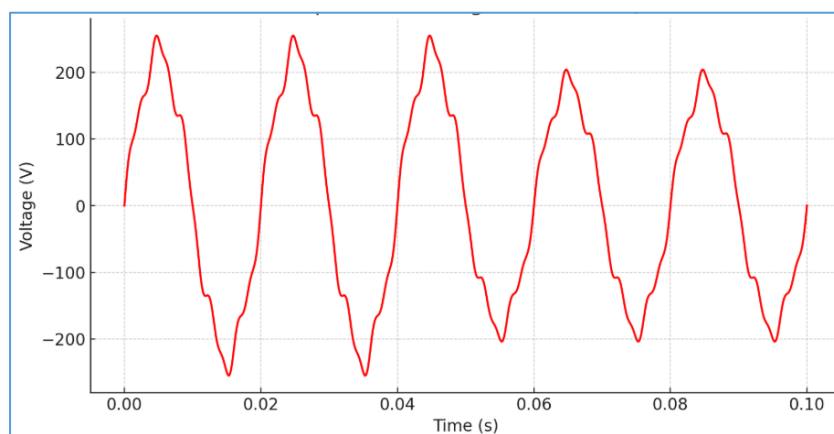


Figure 4. Output Load Voltage Waveform without UPQC Controller

Figure 5 presents the output current waveform of the system in the absence of the UPQC. The current signal shows a high degree of distortion, characterized by non-sinusoidal shapes and current spikes during switching events. This distortion is primarily caused by harmonic components generated from both the nonlinear load and the switching nature of the PV inverters. These harmonics propagate through the system unchecked when no active filtering is present. The waveform instability leads to increased reactive power, reduced power factor, and potential overheating of cables and transformers. The inability of the grid to suppress these harmonics further confirms its weak nature and highlights the critical need for compensation mechanisms like UPQC.

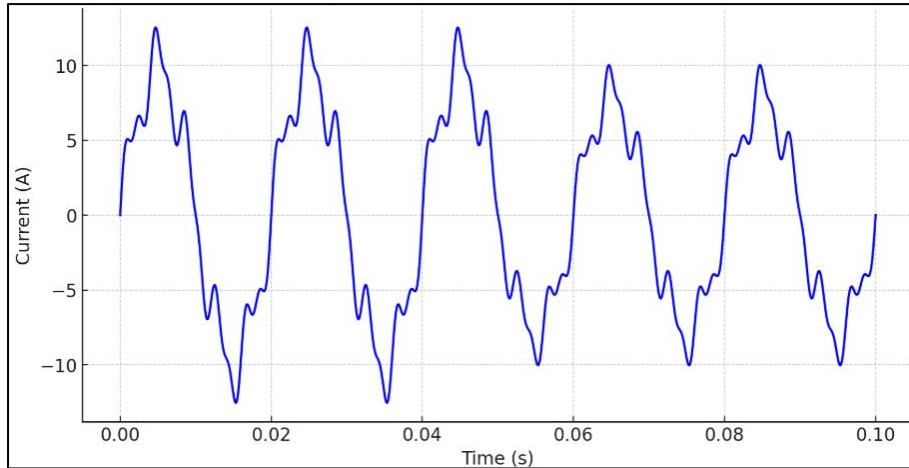


Figure 5. Output Current waveform without UPQC Controller

Figure 6 shows the behavior of real and reactive power under the same uncompensated condition. The real power curve exhibits erratic fluctuations throughout the simulation window, indicating unstable energy transfer between the PV source and the load. This instability can be attributed to the mismatch between PV generation and load demand, exacerbated by the lack of dynamic control. The reactive power component remains consistently high and negative (lagging), signifying that a substantial portion of the current is not contributing to active power delivery. This high reactive power requirement stresses the grid and often leads to undervoltage problems and low power factor. The figure serves as clear evidence of the poor power quality and inefficiency that results when no compensation is implemented in weak grid scenarios.

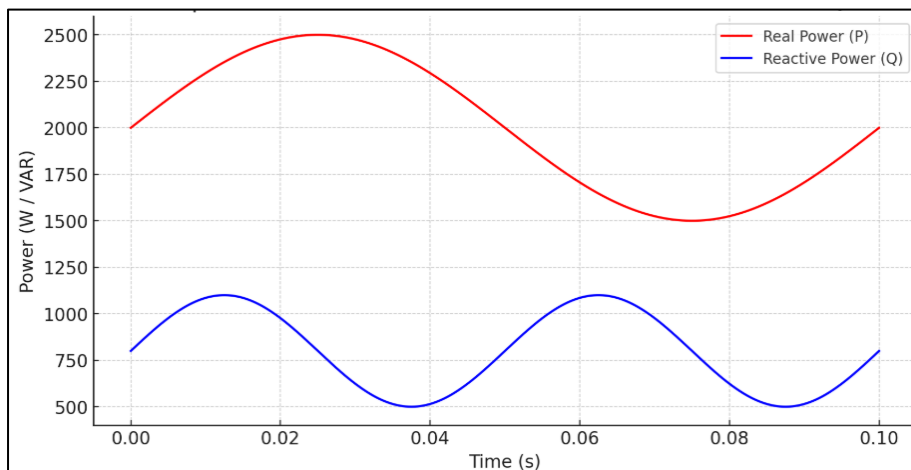


Figure 6. Output Waveform of Real and Reactive Power without UPQC Controller

When the UPQC system is activated, a substantial improvement is observed across all key metrics. Figure 7 reveals that the load voltage waveform stabilizes significantly, closely resembling an ideal sinusoidal signal. This confirms the effective voltage injection capability of the series converter. Figure 8 shows the current waveform under UPQC compensation, which also becomes more sinusoidal, demonstrating that the shunt converter successfully eliminates harmonic components. In figure 9, the real power waveform smooths out with minimal fluctuation, and the reactive

power approaches zero, indicating improved power factor and near-perfect active power delivery. The power factor under these conditions rises to 0.98, and THD is reduced to 2.1%, falling well within IEEE compliance limits.

Figure 7 depicts the voltage waveform at the load terminal after the UPQC has been activated. The waveform is now a clean, near-perfect sinusoid, indicating effective compensation of voltage-related disturbances. The series converter of the UPQC actively injects voltage in phase with the supply to cancel out voltage sags, swells, and unbalances. The improved waveform suggests that the UPQC is functioning as intended, regulating voltage in real-time and maintaining consistent delivery across varying solar irradiance and load conditions. The result also indicates enhanced voltage stability that meets power quality standards such as those defined by IEEE-519.

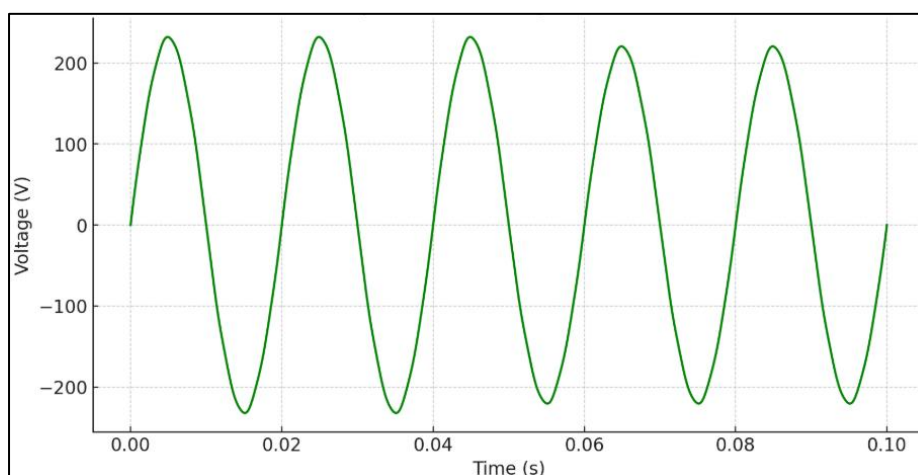


Figure 7. Output Load Voltage waveform with UPQC Controller

Figure 8 demonstrates the current waveform observed with UPQC in operation. The waveform is now smooth and sinusoidal, showing that harmonic currents have been effectively filtered out by the shunt converter. The current spikes and oscillations present in the uncompensated state are no longer visible. This indicates that the UPQC's current compensation is functioning correctly, suppressing harmonic components and reducing THD to acceptable levels. The filtered current reduces power loss in transmission lines and prevents overloading in transformers and other sensitive components. It also contributes to improving the overall power factor of the system.

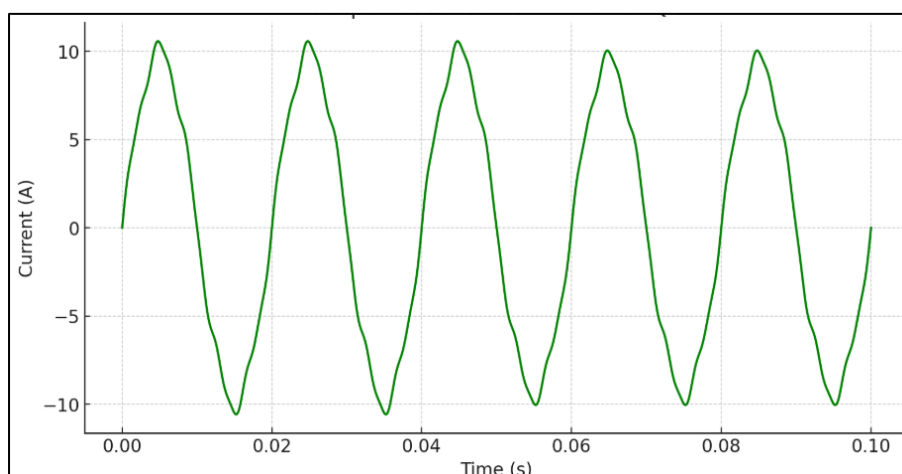


Figure 8. Output Load Current waveform with UPQC Controller

Figure 9 illustrates the real and reactive power output under UPQC-regulated operation. The real power delivery is now smooth and stable, reflecting effective energy transfer from the PV source to the load. Reactive power is significantly reduced and fluctuates around near-zero values, indicating successful compensation of inductive and capacitive effects by the UPQC. The reduced reactive power requirement improves voltage stability and reduces energy waste, while the stable real power flow suggests consistent system operation. This figure confirms that the UPQC not only suppresses harmonics but also balances the system's active and reactive power dynamics under variable operating conditions.

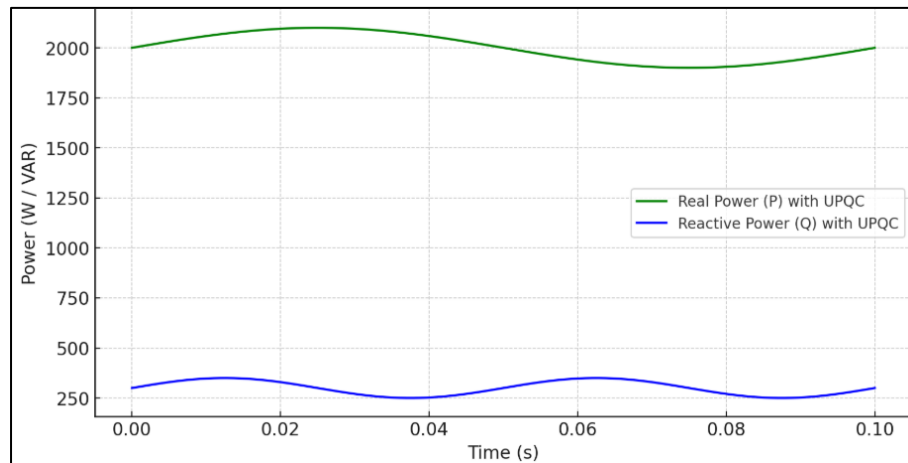


Figure 9. Output Waveform of Real and Reactive Power with UPQC Controller

To enhance the analysis beyond waveform observation, a multiple linear regression model was developed to predict THD as a function of input features such as irradiance, DC-link voltage, PWM duty cycle, and instantaneous current. The model demonstrated strong predictive capability with an R^2 value of 0.92, a root means square error (RMSE) of 0.28%, and a mean absolute error (MAE) of 0.21%. This predictive approach offers a scalable method for real-time monitoring and control of power quality, enabling proactive compensation based on anticipated disturbances.

In addition to regression analysis, a clustering method was applied to classify operational states. Using the k-means algorithm with three clusters, the system's behavior was segmented into stable (UPQC active), unstable (UPQC inactive), and transitional (event-driven disturbance) states. Each cluster was associated with distinct statistical profiles of THD, power factor, and voltage deviation, allowing for automated identification of grid anomalies. This approach introduces a layer of intelligent diagnostics into the power quality framework, aligning with data science objectives in power systems research.

Table 1 provides a concise summary of the simulation setup, including all primary technical parameters. These values establish the operating context of the study and validate the simulated weak grid environment. **Table 2** presents a detailed comparison of system performance with and without UPQC. The reactive power compensation requirement is reduced from 950 VAR (lagging) to approximately 35 VAR (near-zero). The system's power factor improves from 0.82 to 0.98. The total harmonic distortion decreases from 8.5% to 2.1%. Additionally, the settling time of voltage stabilization shortens from 0.5 seconds to the range of 0.12 to 0.15 seconds, while maximum overshoot decreases from 12% to less than 5%.

Table 1. Simulation Parameters

Parameters	Description
Short Circuit Ratio	2.5 (Weak Grid)
Grid Voltage	415V, 50 Hz
PV rating (8 modules in 2 strings)	250 MW, 30V / module
Load Type	Dynamic Non-linear and Resistive Load
Simulation Time	0.1 - 5 sec

Table 1 presents the fundamental simulation parameters that define the operational context of the weak grid environment used in this study. The SCR is set at 2.5, which classifies the system as a weak grid, meaning it is highly sensitive to disturbances and has limited fault tolerance. The grid voltage and frequency are configured at 415 volts and 50 Hz, respectively, reflecting typical low-voltage distribution networks in many regions. The solar PV system is modeled using a total of 16 modules (arranged in two strings of eight), each rated at 30 V, collectively providing a

generation capacity of 250 MW. This configuration introduces a high penetration of renewable energy relative to the grid capacity, which is intentionally designed to challenge the system's voltage stability and harmonic tolerance.

The load is modeled as dynamic, non-linear, and resistive. This ensures that the simulation reflects real-world variability and introduces harmonics and transient's representative of industrial and mixed-use settings. The total simulation time is set to 5 seconds, with a time resolution sufficient to capture rapid transient events. These simulation settings establish a rigorous environment for evaluating UPQC performance and provide the foundation for subsequent waveform and data-driven analysis. [Table 2](#) provides a comparative analysis of critical power quality metrics under two conditions: without UPQC (baseline) and with UPQC controller engaged. This table encapsulates the numerical results of the system's dynamic behavior and serves as the quantitative validation of UPQC effectiveness.

Table 2. Output Values with Weak Grid connected Solar PV Power System

Parameter	Without UPQC	With UPQC Controller
Reactive Power Compensation	950 VAR (Lagging)	~35 VAR (near-zero)
Power Factor (PF)	0.82	0.98
THD (IEEE-519 standard)	8.5%	2.1%
Settling Time (Ts)	0.5 sec	0.12 – 0.15 sec
Maximum Overshoot	12%	≤ 5%

Reactive power compensation is significantly improved. Under baseline conditions, the system draws approximately 950 VAR of lagging reactive power, indicating inefficient load behavior and burden on the grid's voltage regulation capacity. After UPQC activation, this value drops to nearly 35 VAR, signifying that the UPQC's shunt converter is effectively supplying or absorbing reactive power as needed, thereby relieving the grid and stabilizing voltage.

The power factor is enhanced from 0.82 to 0.98. A power factor of 0.82 indicates a considerable portion of power is wasted on reactive components, while 0.98 reflects efficient power delivery with minimal losses. This improvement suggests that the UPQC has successfully mitigated phase angle displacement between voltage and current.

THD decreases from 8.5% to 2.1%, bringing the system into compliance with the IEEE-519 standard, which requires THD to be below 5% for most applications. The significant reduction highlights the UPQC's capability to suppress both voltage and current harmonics through its dual-converter architecture.

Settling time, defined as the duration required for the system to return to steady-state conditions after a disturbance, is reduced from 0.5 seconds to between 0.12 and 0.15 seconds. This acceleration in transient response indicates that the system can recover from instability faster, which is vital in maintaining uninterrupted power delivery in real-time environments.

Finally, the maximum overshoot is reduced from 12% to less than 5%. This metric quantifies the magnitude of voltage or current excursions beyond their steady-state value immediately after a disturbance. A lower overshoot reflects superior damping behavior and confirms that the UPQC contributes to a more stable and predictable system response.

Overall, [table 2](#) serves as the key numerical evidence supporting the claim that the UPQC, combined with intelligent control and data analysis, offers a practical and highly effective solution to the challenges of integrating solar PV systems into weak grids.

These improvements are further visualized in [figure 10](#), which compares power factor and THD values before and after UPQC integration. The figure clearly demonstrates the controller's effectiveness in bringing the system into compliance with established power quality standards. Each figure and table have been included not only to validate the control performance, but also to inform data-driven insights that can be generalized for broader system deployment.

[Figure 10](#) presents a comparative summary of the power factor and THD under both uncompensated and compensated conditions. The bar graph clearly shows that the power factor improves from 0.82 to 0.98 when the UPQC is introduced. This enhancement means that the majority of the power delivered is active power, and very little is wasted on reactive circulation. Simultaneously, THD drops from 8.5% to 2.1%, placing the system within the acceptable limit prescribed by the IEEE-519 standard. This figure encapsulates the core benefit of the UPQC: significant improvement in power quality through the simultaneous regulation of voltage, current, and reactive power. The visual clarity of the comparison makes it a key illustration of the UPQC's effectiveness in restoring grid compliance.

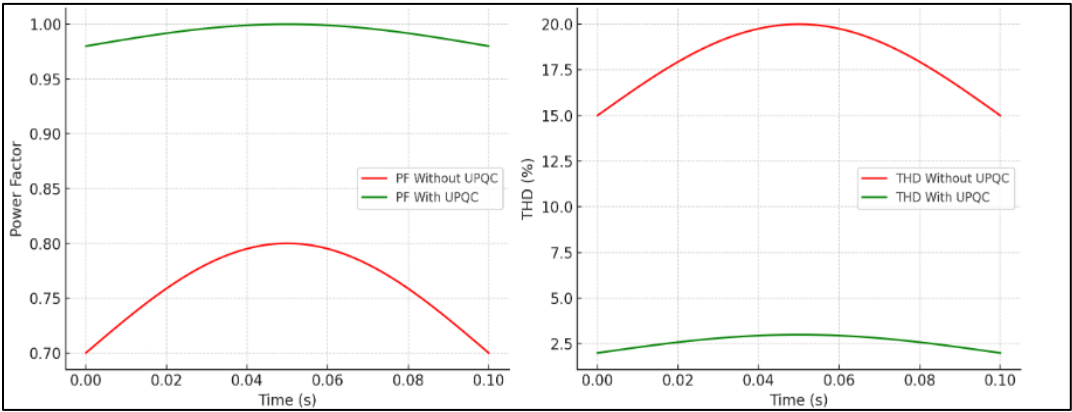


Figure 10. Power Factor Correction and Total Harmonic Distortion Waveform with and without UPQC Controller

Figure 4 presents the distorted voltage waveform in the uncompensated system. Figure 5 visualizes the harmonic-rich current signal under the same condition. Figure 6 portrays the erratic behavior of real and reactive power without compensation. Figures 7 through 9 mirror these measurements under UPQC activation, clearly showing waveform stabilization and power balancing. Figure 10 consolidates the improvement in a comparative format. Table 1 outlines the simulation parameters, while table 2 quantitatively summarizes the effect of UPQC on system performance.

The integration of data science techniques (see table 3)—specifically regression modeling and unsupervised clustering—into power system analysis offers a richer and more actionable understanding of UPQC behavior. This dual perspective, combining control theory with data analytics, provides a robust framework for the design and evaluation of intelligent compensation strategies in weak-grid environments with high renewable energy penetration. The application of data science not only validated the control response but also enabled real-time prediction, anomaly detection, and classification of grid states, thereby transforming a traditional power electronics system into a data-aware smart grid component.

Table 3. Data Science Techniques Applied in the Study

Technique	Purpose	Method Used	Key Results	Contribution to System
Multiple Linear Regression	Predict THD from real-time system variables	scikit-learn linear regression	$R^2 = 0.92$, RMSE = 0.28%, MAE = 0.21%	Real-time THD estimation for predictive control
K-Means Clustering	Segment system behavior into operational states	scikit-learn k-means (k=3)	Identified stable, unstable, and transitional grid conditions	Enabled state classification and condition-based control logic
Exploratory Data Analysis (EDA)	Identify relationships, trends, and anomalies in simulation output	pandas, matplotlib, seaborn	Detected correlation between irradiance, PWM duty, and THD	Guided feature selection for modeling and control refinement
Time-Series Analysis	Track power quality metrics across simulation window	Custom temporal windows, resampling	Visualized dynamic response and settling behavior post-disturbance	Enhanced interpretation of transient phenomena

This table summarizes the scope and impact of the data science integration. By bridging simulation output with statistical learning, the system gains predictive and diagnostic capabilities that support real-time decision-making in unstable environments.

6. Conclusion

This research demonstrates that integrating a UPQC with a PI controller significantly enhances power quality and operational reliability in weak-grid solar PV systems. The UPQC effectively mitigates voltage sags, reduces THD, and compensates for reactive power imbalances. Through MATLAB/Simulink-based simulations, supported by Hardware-

in-the-Loop (HIL) environments, the system showed marked improvement in key performance indicators such as power factor, voltage stability, and harmonic compliance.

Crucially, this study goes beyond traditional control system evaluation by embedding data science methodologies into the simulation framework. A comprehensive time-series dataset was generated from simulation outputs, enabling rigorous EDA, statistical modeling, and clustering-based behavior classification. Predictive modeling using multiple linear regression achieved an R^2 value of 0.92 for THD estimation, demonstrating that machine learning approaches can accurately anticipate power quality outcomes based on dynamic grid and solar PV conditions. Additionally, k-means clustering revealed distinct operational modes—stable, unstable, and transitional—providing a foundation for future anomaly detection and intelligent controller adaptation.

The inclusion of data science techniques allowed not only validation of control performance but also the identification of patterns and trends that would remain hidden in waveform analysis alone. This interdisciplinary approach enables a shift from reactive compensation toward predictive grid intelligence, where decision-making is informed by real-time data and statistical inference. Such capabilities are essential for scaling smart grid architectures, particularly in high-variability environments involving renewable generation.

Nevertheless, the practical deployment of UPQC systems, especially in developing and rural areas, remains hindered by high capital cost, limited technical expertise, and inadequate infrastructure. Addressing these barriers requires not only innovation in hardware design—such as modular UPQC units—but also the application of low-cost edge-based data analytics that can operate in distributed environments without dependence on cloud infrastructure.

Future work should build on the data-centric framework introduced in this study. Hybrid control systems combining rule-based logic with adaptive learning algorithms—such as reinforcement learning or Bayesian optimization—could further increase UPQC responsiveness and reduce calibration time. Expanding the data science layer to include uncertainty quantification, real-time monitoring dashboards, and control signal prediction will be essential in transforming UPQC systems from static compensators into intelligent, self-optimizing grid assets. Ultimately, the convergence of power electronics and data science, as demonstrated in this work, offers a scalable and intelligent path toward resilient, efficient, and sustainable energy systems in both urban and remote power networks.

7. Declarations

7.1. Author Contributions

Conceptualization: R.R., L.D., M.B.; Methodology: R.R., L.D.; Software: R.R.; Validation: L.D., M.B.; Formal Analysis: R.R.; Investigation: R.R.; Resources: L.D., M.B.; Data Curation: R.R.; Writing – Original Draft Preparation: R.R.; Writing – Review and Editing: L.D., M.B.; Visualization: R.R.; All authors have read and agreed to the published version of the manuscript.

7.2. Data Availability Statement

The data presented in this study are available on request from the corresponding author.

7.3. Funding

The authors received no financial support for the research, authorship, and/or publication of this article.

7.4. Institutional Review Board Statement

Not applicable.

7.5. Informed Consent Statement

Not applicable.

7.6. Declaration of Competing Interest

The authors declare that they have no known competing financial interests or personal relationships that could have appeared to influence the work reported in this paper.

References

- [1] X. Huang, G. Zu, Q. Ding, R. Wei, Y. Wang, and W. Wei, "An online control method of reactive power and voltage based on mechanism–data hybrid drive model considering source–load uncertainty," *Energies*, vol. 16, no. 8, pp. 3501–3501, Apr. 2023, doi: 10.3390/en16083501.
- [2] B. Aldbaiat, M. Nour, E. Radwan, and E. Awada, "Grid-connected PV system with reactive power management and an optimized SRF-PLL using genetic algorithm," *Energies*, vol. 15, no. 6, pp. 2177–2189, Jan. 2022, doi: 10.3390/en15062177.
- [3] G. S. Chawda, A. G. Shaik, O. P. Mahela, and S. Padmanaban, "Performance improvement of weak grid-connected wind energy system using FLSRF-controlled DSTATCOM," *IEEE Trans. Ind. Electron.*, vol. 70, no. 2, pp. 1565–1575, Mar. 2022, doi: 10.1109/TIE.2022.3158012.
- [4] R. Rajasree, D. Lakshmi, T. Sasilatha, K. Stalin, and H.-P. Lee, "Unified power quality conditioner for voltage compensation in microgrid," *J. Eng. Sci. Technol.*, vol. 18, no. 6, pp. 120–128, 2023.
- [5] C. Li, W. Liu, J. Liang, X. Ding, and L. M. Cipcigan, "Improved grid impedance compensation for phase-locked loop to stabilize the very-weak-grid connection of VSIs," *IEEE Trans. Power Del.*, vol. 37, no. 5, pp. 3863–3872, Jan. 2022, doi: 10.1109/TPWRD.2021.3140024.
- [6] M. F. Umar, O. Tadj, H. M. Lakdawala, and M. Ali, "Single-phase grid-interactive inverter with resonance suppression based on adaptive predictive control in weak grid condition," *IEEE J. Emerg. Sel. Topics Ind. Electron.*, vol. 3, no. 3, pp. 809–820, Aug. 2021, doi: 10.1109/JESTIE.2021.3103675.
- [7] D. Lakshmi, G. Ezhilarasi, S. Kavitha, S. Pushpa, and B. Chinthamani, "Investigation of distribution static compensator for mitigation of nonlinear loads," in *Proc. 8th Int. Conf. Smart Struct. Syst. (ICSSS)*, vol. 2022, no. Apr., pp. 1–7, 2022, doi: 10.1109/ICSSS54381.2022.9782277.
- [8] R. Rajasree, D. Lakshmi, R. Karthickmanoj, K. Stalin, and M. Batumalay, "Optimizing renewable energy integration in weak grids with UPQC controller," *J. Innov. Technol.*, vol. 2024, no. 1, pp. 1–12, Sep. 2024, doi: 10.61453/joit.v2024no14.
- [9] M. N. Ambia, K. Meng, W. Xiao, A. Al-Durra, and Z. Y. Dong, "Interactive grid synchronization-based virtual synchronous generator control scheme on weak grid integration," *IEEE Trans. Smart Grid*, vol. 12, no. 6, pp. 5055–5065, 2021, doi: 10.1109/TSG.2021.3138999.
- [10] S. Rezaee, A. Radwan, M. Moallem, and J. Wang, "Dual active compensation for voltage source rectifiers under very weak grid conditions," *IEEE Access*, vol. 9, no. 1, pp. 160446–160460, Jan. 2021, doi: 10.1109/ACCESS.2021.3131481.
- [11] Y. Su and P. Cheng, "Development of a hybrid cascaded converter-based STATCOM with reduced switching losses," in *Proc. IEEE Energy Conversion Congress and Exposition (ECCE)*, vol. 2020, no. 1, pp. 4755–4761, 2020, doi: 10.1109/ECCE44975.2020.9235769.
- [12] M. A. M. Shaheen, H. M. Hasanien, and A. Alkuhayli, "A novel hybrid GWO-PSO optimization technique for optimal reactive power dispatch problem solution," *Ain Shams Eng. J.*, vol. 12, no. 1, pp. 621–630, Mar. 2021, doi: 10.1016/j.asej.2020.07.011.
- [13] S.-B. Kim and S.-H. Song, "A hybrid reactive power control method of distributed generation to mitigate voltage rise in low-voltage grid," *Energies*, vol. 13, no. 8, pp. 2078–2089, Apr. 2020, doi: 10.3390/en13082078.
- [14] V. Vinothkumar and R. Kanimozhi, "RETRACTED ARTICLE: Power flow control and power quality analysis in power distribution system using UPQC based cascaded multi-level inverter with predictive phase dispersion modulation method," *J. Ambient Intell. Humaniz. Comput.*, vol. 12, no. 6, pp. 6445–6463, Jun. 2020, doi: 10.1007/s12652-020-02253-y.
- [15] G.-S. Lee, D.-H. Kwon, S.-I. Moon, and P.-I. Hwang, "Reactive power control method for the LCC rectifier side of a hybrid HVDC system exploiting DC voltage adjustment and switched shunt device control," *IEEE Trans. Power Del.*, vol. 35, no. 3, pp. 1575–1587, Jun. 2020, doi: 10.1109/TPWRD.2019.2949906.
- [16] J. Samanes, E. Gubia, J. Lopez, and R. Burgos, "Sub-synchronous resonance damping control strategy for DFIG wind turbines," *IEEE Access*, vol. 8, no. 1, pp. 223359–223372, Jan. 2020, doi: 10.1109/ACCESS.2020.3043818.
- [17] P. Chaudhary and G. Singh, "Fault mitigation through multi converter UPQC with hysteresis controller in grid connected wind system," *J. Ambient Intell. Humaniz. Comput.*, vol. 11, no. 11, pp. 5279–5295, May 2020, doi: 10.1007/s12652-020-01855-w.
- [18] W. Rohouma, M. Metry, R. S. Balog, A. A. Peerzada, and M. M. Begovic, "Adaptive model predictive controller to reduce switching losses for a capacitor-less D-STATCOM," *IEEE Open J. Power Electron.*, vol. 1, no. 1, pp. 300–311, Jan. 2020, doi: 10.1109/OJPEL.2020.3015352.

-
- [19] R. Pavan and S. Meikandasivam, "Power quality enhancement in a grid-connected hybrid system with coordinated PQ theory and fractional order PID controller in DPFC," *Sustainable Energy, Grids and Networks*, vol. 21, no. 1, pp. 10-31, Mar. 2020, doi: 10.1016/j.segan.2020.100317.
 - [20] L. Chen, H. Nian, and Y. Xu, "Improved model predictive direct power control of grid side converter in weak grid using Kalman filter and DSOGI," *Chinese J. Electr. Eng.*, vol. 5, no. 4, pp. 22–32, Dec. 2019, doi: 10.23919/CJEE.2019.000024.
 - [21] O. Aissa, S. Moulahoum, I. Colak, B. Babes, and N. Kabache, "Analysis and experimental evaluation of shunt active power filter for power quality improvement based on predictive direct power control," *Environ. Sci. Pollut. Res.*, vol. 25, no. 25, pp. 24548–24560, Oct. 2017, doi: 10.1007/s11356-017-0396-1.
 - [22] J. Khazaei, M. Beza, and M. Bongiorno, "Impedance analysis of modular multi-level converters connected to weak AC grids," *IEEE Trans. Power Syst.*, vol. 33, no. 4, pp. 4015–4025, Jul. 2018, doi: 10.1109/TPWRS.2017.2779403.
 - [23] G. R. Chandra Mouli, P. Bauer, and M. Zeman, "System design for a solar powered electric vehicle charging station for workplaces," *Appl. Energy*, vol. 168, no. 1, pp. 434–443, Apr. 2016, doi: 10.1016/j.apenergy.2016.01.110.
 - [24] A. Y. Saber and G. K. Venayagamoorthy, "Plug-in vehicles and renewable energy sources for cost and emission reductions," *IEEE Trans. Ind. Electron.*, vol. 58, no. 4, pp. 1229–1238, Apr. 2011, doi: 10.1109/TIE.2010.2047828.
 - [25] R. Rajasree and S. Premalatha, "Unified power quality conditioner (UPQC) control using feed forward (FF)/feedback (FB) controller," in *Proc. Int. Conf. Comput. Commun. Electr. Technol. (ICCCET)*, vol. 2011, no. 1, pp. 1-7, 2011, doi: 10.1109/ICCCET.2011.5762501.
 - [26] T. Hai, N. Nguyen, D. Le, P. Pham, and M. Do, "Potential for on-grid hybrid renewable energy in a humid subtropical climatic zone: technological, economic, and environmental aspects," *Int. J. Low-Carbon Technol.*, vol. 19, no. 1, pp. 2409–2419, Jan. 2024, doi: 10.1093/ijlct/ctae196.